Proc. Natl. Acad. Sci. USA
Vol. 93, pp. 4459–4464, April 1996
Biophysics

The neck region of the myosin motor domain acts as a lever arm to generate movement

TARO Q. P. UYEDA*, PAUL D. ABRAMSON†, AND JAMES A. SPUDICH†

*Bionic Design Group, National Institute for Advanced Interdisciplinary Research and Mechanical Engineering Laboratory, Agency of Industrial Science and Technology, Tsukuba, Ibaraki 305, Japan; and †Department of Biochemistry, Stanford University School of Medicine, Stanford, CA 94305

Contributed by James A. Spudich, January 4, 1996

ABSTRACT **The myosin head consists of a globular catalytic domain that binds actin and hydrolyzes ATP and a neck domain that consists of essential and regulatory light chains bound to a long α-helical portion of the heavy chain. The swinging neck-lever model assumes that a swinging motion of the neck relative to the catalytic domain is the origin of movement. This model predicts that the step size, and consequently the sliding velocity, are linearly related to the length of the neck. We have tested this point by characterizing a series of mutant *Dictyostelium* myosins that have different neck lengths. The 2xELCBS mutant has an extra binding site for essential light chain. The ΔRLCBS mutant myosin has an internal deletion that removes the regulatory light chain binding site. The ΔBLCBS mutant lacks both light chain binding sites. Wild-type myosin and these mutant myosins were subjected to the sliding filament *in vitro* motility assay. As expected, mutants with shorter necks move slower than wild-type myosin *in vitro*. Most significantly, a mutant with a longer neck moves faster than the wild type, and the sliding velocities of these myosins are linearly related to the neck length, as predicted by the swinging neck-lever model. A simple extrapolation to zero speed predicts that the fulcrum point is in the vicinity of the SH1–SH2 region in the catalytic domain.**

The conventional myosin or myosin II, referred to as simply myosin throughout, is a hexamer that consists of two identical heavy chains and two pairs of essential and regulatory light chains (ELC and RLC). The amino-terminal 87 kDa of each heavy chain forms the catalytic domain, which contains the ATPase and actin-binding activities (1). Carboxyl to the catalytic domain, the heavy chain forms a single α-helix of ≈8 nm, and each of the two light chains wraps around this α-helix, forming the neck domain (2, 3). A currently prevailing model assumes that an intramolecular conformational change within the myosin head causes relative displacement between actin and myosin (4, 5). The three-dimensional (3-D) structure of the head provided a structural basis for this model by suggesting that the neck domain swings relative to the catalytic domain and generates movement like a lever arm (the swinging neck-lever model) (2) (Fig. 1 *Upper*). Depending on the magnitude of the angle change, the swinging motion of the ≈8-nm-long lever arm could produce a displacement of similar size, in keeping with 4- to 10-nm steps directly measured (6–9).

Electron microscopy has successfully observed two different shapes of the head in a way that is consistent with this model (10). Physical measurements have also supported this hypothesis by demonstrating a cyclic change in gyratory radius of the head during ATP hydrolysis cycles (11, 12). Recently, 3-D helical reconstruction of actin decorated with myosin heads revealed a swinging motion of the neck region associated with release of ADP from the catalytic domain, resulting in 3- to 4-nm displacements at the distal end of the neck region (13, 14). However, a caveat of these earlier studies is that the experiments were done in solutions under the conditions of no load or restraining force, and it was not clear if the conformational change is capable of generating contractile force. Irving *et al.* (15) detected an angle change of the neck region in synchronized muscle fibers using a fluorescence polarization technique, but the observed angle change using this technique appeared too small to generate 5- to 10-nm steps. Thus, the swinging neck-lever model has remained controversial.

A direct prediction of the swinging neck-lever model is that the size of the displacement produced by each stroke is proportional to the length of the neck domain. It is assumed that this stroke occurs while the actin-myosin complex is in its strongly bound state, and, in the sliding filament *in vitro* motility assay, the average sliding velocity (v) is primarily determined by the stroke size (d) divided by the strongly bound state time (t_s) (16–18). Thus, the above prediction can be translated to a linear relationship between the average sliding velocity and the neck length, assuming that t_s is constant. A number of studies have indeed shown that myosin or its fragments with shorter or less rigid lever arms move more slowly than wild-type myosin *in vitro* (1, 19–21). While suggestive, it is difficult to interpret mutations that give rise to diminished function compared with wild type. We therefore set out to systematically change the length of the lever arm of *Dictyostelium* myosin, including making it longer, to examine whether there is a linear relationship between lever arm length and velocity *in vitro*.

MATERIALS AND METHODS

Plasmid Construction and Site-Directed Mutagenesis. Standard methods were used for all DNA manipulations (22). The template for mutagenesis was pMyDAP (23), which carries the entire myosin heavy chain gene fused to the actin 15 promoter. ΔBLCBS heavy chain was made by using a PCR-based method as described (20). The sequence of the mutagenic primer was 5′-CGTATTGAAGAAGCACGTGAACAACGTCCATTATTAAAGAGAAG. Mutant 2xELCBS was made by inserting an ELC binding site, as follows. A silent mutation was first made at the unique *Acc* I site within the ELC binding site to change GTCTAC to GTATAC, a recognition sequence of the blunt cutter *Bst*1107I. An ELC binding site sequence was synthesized by the mutual priming method (22). Sequence of the product is TATAAGCAAGAAAGAATCAGCGAAATTATCAAGGCTATCCAAGCCGCTACAAGAGGATGGATTGCCAGAAAGGTA. This was inserted at the *Bst*1107I site, and a clone with the correct orientation was selected. The mutant myosin heavy chain genes were sequenced and subcloned into pTIKL, a pBIG-derived (24) extrachromosomal vector carrying a G418-resistance gene. Mutant ΔRLCBS, which lacks only the RLC

The publication costs of this article were defrayed in part by page charge payment. This article must therefore be hereby marked "*advertisement*" in accordance with 18 U.S.C. §1734 solely to indicate this fact.

Abbreviations: ELC, essential light chain; RLC, regulatory light chain; 3-D, three-dimensional.

binding site, was engineered and has been characterized previously (20).

Manipulation of *Dictyostelium* Cells. HS1, a mutant cell line of *Dictyostelium discoideum* that lacks the endogenous myosin heavy chain gene, was created by Ruppel *et al.* (24) and was maintained on plastic dishes containing HL5 medium (25) supplemented with 60 μg each of penicillin and streptomycin per ml (HL5PS medium). The cells were transfected with pTIKL carrying each one of the mutant or wild-type myosin heavy chain genes by electroporation (26). Independent transformants were selected in HL5PS medium in the presence of 12 μg of G418 per ml and were maintained in the same medium at 21–22°C.

Preparation of Proteins. For the isolation of *Dictyostelium* myosin, the cells expressing one of each mutant or wild-type myosin were grown in six-liter flasks containing 2.5 liter of HL5PS supplemented with 12 μg of G418 per ml on a rotary shaker at 22°C. Myosins were then purified by the method described previously (20).

Rabbit skeletal muscle actin and myosin were prepared by the method of Spudich and Watt (27) and Margossian and Lowey (28), respectively. The concentrations of these proteins were determined spectrophotometrically using extinction coefficients of 0.62 cm^2/mg at 290 nm for actin (29) and 0.53 cm^2/mg at 280 nm for myosin (28). The concentration of purified *Dictyostelium* myosin was measured by the method of Bradford (30) with rabbit skeletal muscle myosin as the standard.

ATPase Assays. The purified mutant and wild-type myosins were incubated in 2 mM ATP/3 mM $MgCl_2$/50 mM NaCl/1 mM dithiothreitol/10 mM Hepes, pH 7.4, for 30 min at 22°C in the presence or absence of 0.1 mg of recombinant *Dictyostelium* myosin light chain kinase per ml (24). The degree of RLC phosphorylation was examined by urea/SDS/glycerol polyacrylamide gel electrophoresis performed according to a modified method (24) of Perrie and Perry (31). The treated myosin was precipitated by centrifugation at 75,000 rpm in a Beckman TL100.3 rotor for 20 min and dissolved in 200 mM

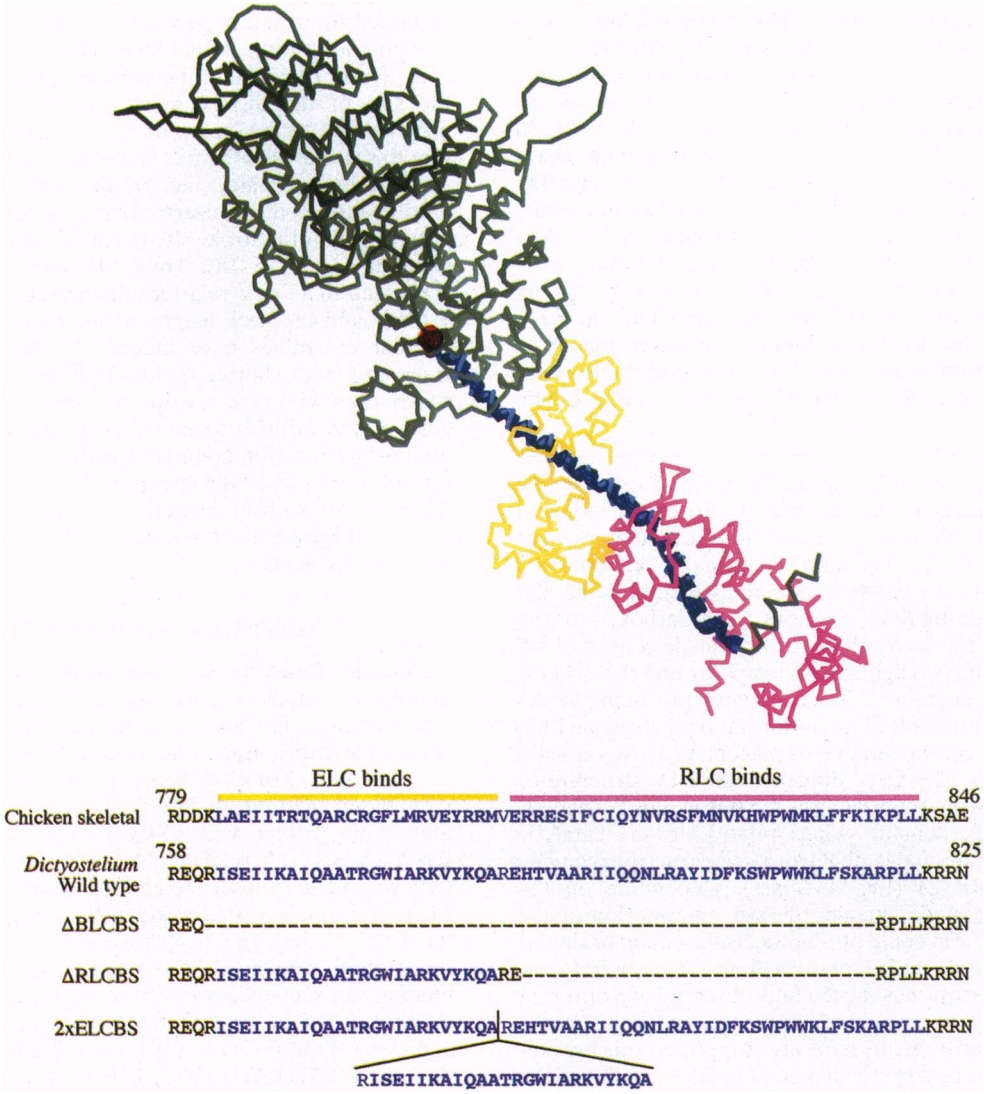

FIG. 1. (*Upper*) Chicken S1 structure of Rayment *et al.* (2), modified to include missing residues by M. Lorenz (personal communication). The actin filament (not shown) would run vertically within the plane of the paper and interact with the myosin at the actin-binding face at the upper left. The "catalytic domain" is shown in black, while the C-terminal part of the heavy chain portion of S1 forms an ≈8-nm-long α-helix (violet), which binds both the essential (yellow) and regulatory (pink) light chains, giving rise to the "neck domain." The ATP- and actin-binding sites are on opposite sides of the globular catalytic domain. The red dot indicates the position of a putative fulcrum point for the relative movement of the lever arm and the catalytic domain. (*Lower*) Partial amino acid sequence of chicken skeletal (34) and *Dictyostelium* (35) myosin heavy chains. Chicken ELC and RLC binding sites, as deduced from the atomic structure (2), and corresponding residues of the *Dictyostelium* sequence, are shown in violet. Sequences of mutant heavy chains used in this study are shown below.

KCl/1 mM dithiothreitol/10 mM Hepes, pH 7.4. The resultant myosin solution was adjusted to conform to the following final ATPase assay conditions, with myosin at 0.1 mg/ml (24): the high-salt CaATPase assay condition, 10 mM imidazole, pH 7.4/0.6 M KCl/5 mM $CaCl_2$/1 mM dithiothreitol; the MgATPase assay condition, 10 mM imidazole, pH 7.4/25 mM KCl/4 mM $MgCl_2$/1 mM dithiothreitol and with or without 1 mg of rabbit skeletal muscle F-actin per ml. The reaction was started by adding 3 mM [γ-^{32}P]ATP and was allowed to proceed for 21 min at 30°C.

***In Vitro* Motility Assay.** Sliding filament *in vitro* motility assays were performed at 30°C on nitrocellulose surfaces (32, 33). Phosphorylated myosin in 200 mM KCl/1 mM dithiothreitol/10 mM Hepes, pH 7.4, was centrifuged at 55,000 rpm for 2 min in a Beckman TL100.1 rotor immediately after the addition of 0.1 mg of rabbit skeletal muscle F-actin per ml and 2 mM MgATP to remove denatured molecules that bind irreversibly to actin (41). Prior to introduction of fluorescently labeled F-actin, myosin-coated flow cells were treated with unlabeled F-actin and MgATP in order to "block" residual denatured molecules. Velocities of at least 43 filaments were scored for each myosin, after elimination of filaments whose segmental velocity deviated >25% from the average among several segments of a run longer than 2–3 s (for slower myosins) or 3–5 μm (for faster myosins). These sample pretreatments and careful selection of smoothly moving filaments resulted in somewhat faster average sliding velocities with similar standard deviation compared to our earlier reports (20, 24).

RESULTS AND DISCUSSION

The structure of the neck domain (2, 3) makes it relatively straightforward in *Dictyostelium* to design mutant heavy chain genes of different neck length by deleting or inserting light chain binding site(s) (Fig. 1). Based on this strategy, we have made the following mutant myosin heavy chain genes of *Dictyostelium*: ΔBLCBS (lacks both light chain binding sites), ΔRLCBS (lacks the RLC binding site only), and 2xELCBS (has an extra binding site for the ELC) (Fig. 1 *Lower*).

These mutant myosins were expressed individually in *Dictyostelium* cells that lack the endogenous copy of the myosin heavy chain gene (24) and were purified for *in vitro* analysis. Coomassie-stained SDS/PAGE gels demonstrated that deletion of light chain binding sites resulted in loss of appropriate light chains (Fig. 2). 2xELCBS myosin was associated with more ELC peptide when compared with wild type. Densitometric scanning quantitation showed that 2xELCBS, compared with wild type, was associated with 70% more ELC when normalized against the intensity of the RLC band. Thus, 70% of the total 2xELCBS heavy chains had both ELC binding sites occupied with the ELC peptide, assuming that all of the original sites were occupied.

Table 1. ATPase activities of mutant and wild-type myosins

Myosin	Kinase treatment	High-salt CaATPase	MgATPase	
			− actin	+ actin
ΔBLCBS	−	1.6	ND	1.4
	−	2.0	0.074	1.3
ΔRLCBS	−	4.0	ND	1.6
	−	4.0	0.13	1.3
Wild type	−	2.4	ND	0.16
	−	2.1	0.001	0.14
	+	ND	ND	0.63
	+	ND	0.038	0.72
2xELCBS	−	3.2	ND	1.1
	−	3.8	0.13	1.2
	+	ND	ND	1.2
	+	ND	0.13	1.4

The ATPase activities of kinase-treated or untreated myosins were measured at 30°C. The results of two independent preparations are shown as P_i liberated per head per s. ND, not determined.

Aliquots of purified myosins were treated with myosin light chain kinase, and the ATPase activities were measured. All mutants showed nearly the same actin-activated myosin ATPase activities, and these were about 2-fold higher than for wild-type myosin (Table 1). Furthermore, not only the ΔRLCBS and ΔBLCBS mutants, which lack RLC itself, but also the 2xELCBS mutant was no longer regulated by treatment with the myosin light chain kinase. Urea/SDS/glycerol PAGE analysis was used to separate phosphorylated and dephosphorylated RLC and to determine the percent phosphorylation in each myosin sample (Fig. 3) (24). Those myosin samples not treated with myosin light chain kinase were <10% phosphorylated, while those treated with kinase were >90% phosphorylated. Thus, the high actin-activated ATPase activity of 2xELCBS in the absence of kinase treatment is not due to a high level of endogenous RLC phosphorylation. Presumably the altered context of interaction between the catalytic domain and RLC abolished the regulation by RLC phosphorylation.

It should be noted that the elevation in ATPase rate is not connected to a necessary change in velocity, since ATPase and velocity are limited by different rate-limiting steps. The rate limiting step of the actin-activated MgATPase cycle involves some transition between weakly bound states of myosin (36,

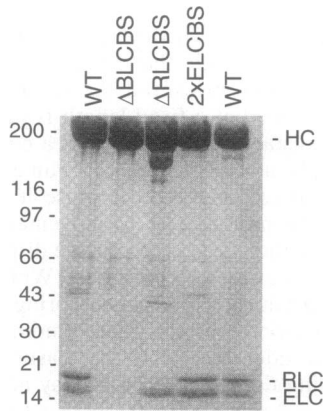

FIG. 2. SDS/PAGE analysis of purified mutant and wild-type myosins. Approximately 10 μg of each purified myosin was loaded on a 15% acrylamide gel. The two lanes with wild-type (WT) myosin show different preparations. The heavy chain of ΔRLCBS is partially nicked in this particular preparation, but identical results were obtained with undegraded preparations. HC, myosin heavy chain.

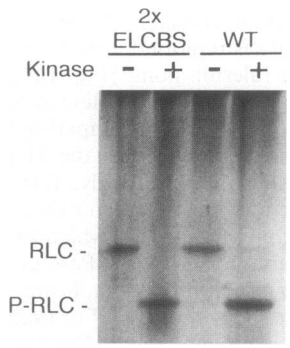

FIG. 3. Urea/SDS/glycerol PAGE to resolve phosphorylated and dephosphorylated RLC. Wild-type (WT) and mutant 2xELCBS myosins were incubated in MgATP with or without *Dictyostelium* myosin light chain kinase as described in *Materials and Methods*, and ≈20 μg of each protein was loaded. RLC, dephosphorylated RLC; P-RLC, phosphorylated RLC.

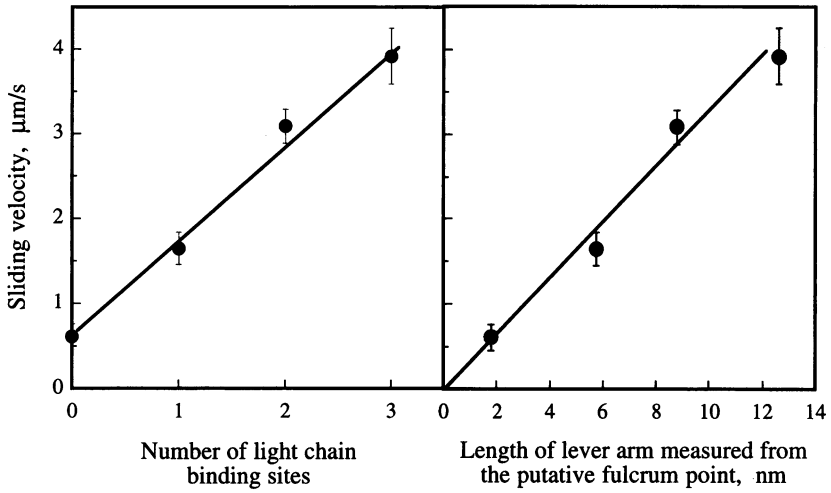

FIG. 4. Sliding velocities of mutant and wild-type myosins. Bars indicate standard deviation. (*Left*) Sliding velocity as a function of the number of light chain binding sites. These data are representative of four independent experiments with different preparations of proteins over a period of a year. (*Right*) The same set of data is replotted against the length of the putative lever arm. The lever arm lengths for wild type and each mutant were measured from the fulcrum point shown as a red dot in Fig. 1 to the ≈90° bend at the C terminus of the long heavy chain α-helix (shown in violet in Fig. 1) that makes up the neck domain—these lengths are 3-D computer-graphic measurements based on the crystal structure (2).

37), while the strongly bound state time, t_s, determines the velocity at which movement occurs (16–18). Thus, the elevated ATPase is not a reflection of a change in t_s and thus is not relevant to velocity considerations. Importantly, we can conclude that none of the mutated myosins have been hampered in their ability to hydrolyze ATP, which we take as an indication that the mutations did not have generally deleterious effects on the myosin.

The mutant and wild-type myosins were then subjected to an *in vitro* sliding filament motility assay (32, 33, 41). The sliding velocities increased with increasing number of light chain binding sites for wild-type and mutant myosins (Fig. 4 *Left*), consistent with the swinging neck-lever model. Most significantly, the 2xELCBS mutant form moved faster than the wild-type myosin (the range was 21–33% faster in four experiments), and the most straightforward interpretation of making the enzyme move faster is that the neck behaves like a lever arm.

If one makes the further (undoubtedly oversimplified) assumptions that, first, all of the stroke derives from the movement of a relatively rigid lever arm that rotates about some fulcrum point, and, second, that the 2xELCBS mutant has a lever arm that is elongated by the linear insertion of one extra ELC binding domain, then one can extrapolate the points in Fig. 4 *Left* back to zero lever arm length. This "fulcrum point" in the structure is shown by the red dot in Fig. 1, and the sliding velocities are now proportional to the length of lever arm when the same set of data is replotted against the length measured from this putative fulcrum point (Fig. 4 *Right*). Milligan and colleagues (13, 14) provided complementary evidence for a fulcrum point in this region by comparing helically reconstituted actomyosin structures between the ADP-bound and rigor (no nucleotide) states. Interestingly, this putative fulcrum point is very near to what has been called the reactive thiol region in skeletal muscle myosin, which undergoes dramatic changes in structure during the ATPase cycle (38, 39).

There are other, albeit more complicated, explanations for the velocity results shown in Fig. 4. For example, it is possible that there is another minor but independent mechanism to generate movement, such as a change in binding angle between actin and the myosin head at the actin–myosin binding face, as has been long postulated (40). Thus, the fulcrum point of the swinging motion of the lever arm may be to the right of the red dot in Fig. 1 *Upper*, closer to the ELC binding domain. Another possibility is that t_s is linearly related to the number of light chain binding sites, and this contributes to the changes in velocity since $v = d/t_s$. This possibility can be tested in the future. For example, the feedback-enhanced laser trap assay (6) can be used to determine t_s directly as a measure of the duration time of the myosin displacement.

In summary, the linear relationship between sliding velocity and the neck length strongly supports the swinging neck-lever model. It is particularly noteworthy that we were able to create a mutant motor that moves faster than the wild type in a way the model predicts. An interesting point to consider (see *Appendix*) is that this lever arm of the S1 will have a certain bending stiffness and may be the structural equivalent of the elastic element that has long been known to be part of the actin–myosin system, as elucidated by tension-transient experiments using muscle fibers (40).

APPENDIX: Is the lever arm of myosin a molecular elastic element?

JONATHON HOWARD* AND JAMES A. SPUDICH†

*Department of Physiology and Biophysics, University of Washington, Seattle, WA 98195-7290; and †Department of Biochemistry, Stanford University School of Medicine, Stanford, CA 94305

The classic experiments of Huxley and Simmons (40) defined an elastic element in muscle that has been attributed to the myosin molecule. They measured the tension drop when a stimulated muscle held at a fixed length is rapidly shortened through a small distance and found that a component of the system behaves like a linear spring. Such an elastic element is fundamental to force generation because it allows strain to develop within the motor prior to movement of the cargo; relief of this strain then drives the relative displacement of the motor and the track along which it moves. While diagrammatic representations often show this elastic spring as being part of the myosin rod beyond the light-chain binding domain of the molecule, we consider here that the elastic element is the light-chain binding domain itself and may account quantitatively for the cross-bridge stiffness observed in muscle experiments.

The head domain of myosin, commonly called subfragment 1 or S1, is the only part of the myosin molecule required for movement *in vitro* (33) and for production of force similar to that seen in intact muscle (9, 42). An unusual structural feature of S1 is the ≈18-nm-long light-chain binding domain that is at

the C terminus of the S1 moiety (2, 3). It has been suggested that this region of the myosin head could serve as a lever arm to amplify smaller conformational changes elsewhere in the motor domain (5, 13–15, 19–21, 43, and this paper). Indeed, fluorescence polarization experiments have shown that the light-chain binding region changes orientation by a minimum of 3° relative to the filament axis in muscle in response to quick length changes and during the transitions between states of the cross-bridge cycle associated with active force production (15). While this angle change would appear to be too small to account for a unitary displacement of several nanometers (6), it is a minimum value for technical reasons, and two other complementary studies strongly support the lever arm hypothesis. First, electron microscopy of decorated actin filaments showed that a rotation of the light-chain binding domain through ≈23° accounts well for the two different conformations that S1 adopts depending on whether ADP is bound at the active site; the difference could account for as much as 3.5 nm of movement of the far C terminus of S1 (13, 14). Second, this paper used molecular genetic approaches to shorten, and importantly, to elongate the lever arm and demonstrate a linear relationship between the lever arm length and the velocity with which the myosin moves *in vitro*.

We argue here that the lever arm could also be the elastic element referred to above, since the elasticity of the light-chain binding domain is expected to be comparable to that measured in the rapid shortening experiments. Furthermore, the nature of the light chains and their interaction with the ≈8-nm-long α-helical stretch of the heavy chain at the C terminus of S1 may determine the spring constant of the light-chain binding domain and therefore affect the force that the molecular motor can produce.

Consider a very simple model of the lever arm as a clamped beam of length L and flexural rigidity (the resistance to bending forces) equal to EI. If a transverse force F is applied at the free end, then this end will move through a distance x such that:

$$F = (3EI/L^3)x$$

(44). In other words, the beam has a stiffness

$$\kappa = 3EI/L^3 = 3kTL_p/L^3,$$

where $L_p = EI/kT$ is the persistence length (45), k is the Boltzmann constant, and T is temperature. The light-chain binding domain has a length of ≈8 nm. It seems reasonable to consider that the lever arm, which has two light chains wrapped around the long α-helix, has a rigidity similar to that of a coiled coil, which has two α-helices wrapped around each other. The persistence length of a coiled coil is ≈100 nm (J.H., unpublished measurements derived from the coiled-coil myosin rod domain). For comparison, the L_p of DNA, which has a dimension similar to these two protein structures, is ≈50 nm (46). Substituting L = 8 nm, L_p = 100 nm, and kT = 4 pN·nm, we obtain

$$\kappa \approx 2 \text{ pN/nm}.$$

On the other hand, the rapid shortening experiments indicate a muscle stiffness equal to 0.27 pN/nm when normalized to the total number of myosin heads per half sarcomere [a shortening of 6 nm per half sarcomere drops the force from 1.6 pN per head to zero (47)]. Since only about half the compliance in muscle resides in the myosin heads and the other half resides in the actin filaments (e.g., see ref. 48), this value for the stiffness needs to be doubled to ≈0.5 pN/nm per myosin head. If only a quarter of the myosin heads were attached during isometric contraction (duty ratio of ≈0.25; refs. 6 and 16), then the stiffness per attached head would be ≈2 pN/nm, equal to that derived above! Clearly, this equality could be fortuitous given the large uncertainties in both the experimental and theoretical stiffnesses. The assumptions made, however, are not unreasonable, and the calculations do show that it is quite plausible that the elasticity of myosin resides within the light-chain binding domain, which corresponds to the lever arm. Indeed, one expects the light-chain binding domain to contribute some compliance to the myosin molecule.

There are three interesting predictions that follow from the hypothesis that the lever arm is the elastic element.

(*i*) The motor force should be inversely proportional to the square of the length of the lever arm. To see this, let the force-generating conformational change be a rotation, through an angle $\Delta\theta$, of the insertion point of the lever into the motor domain. Thus, in the absence of a restoring force, the tip of the lever arm (the C terminus of S1) would move through a distance

$$\Delta x = L\Delta\theta.$$

On the other hand if there were a restoring force (F_{max}) that prevented the C terminus of the lever arm from moving, then

$$F_{max} = (3kTL_p/L^3)\Delta x = (3kTL_p/L^3)\, L\Delta\theta = 3kTL_p\Delta\theta/L^2.$$

Since the angular change $\Delta\theta$ is independent of the length of the lever arm, it follows that the maximum force is proportional to L^{-2}. On the other hand, if the lever arm acted as a rigid rod and the elasticity were due to a pivotal spring (49) located at the point of insertion into the motor domain, then the maximum force would depend on L^{-1}.

(*ii*) The maximum work should be inversely proportional to the lever length (L^{-1}). To see this, note that if the restoring force (F_o) is less than the maximum force, then the tip will move through a distance

$$\Delta x - F_o/\kappa \text{ (the working stroke)},$$

and the amount of work done will equal

$$W = F_o(\Delta x - F_o/\kappa) = F_o\Delta x - F_o^2/\kappa.$$

The maximum work occurs when $F_o = F_{max}/2$, and

$$W_{max} = F_{max}\Delta x/4 = (3/4)kTL_p\Delta\theta^2/L.$$

That is, the maximum work is inversely proportional to the lever length. This leads to a paradox at the shortest lever arm lengths where the work might get so large as to exceed the theoretical maximum force. Presumably a motor with a very short lever arm will fail at high forces (the rotation through $\Delta\theta$ would not take place).

(*iii*) The maximum force will depend on the stiffness of the lever arm. For example, if the link between the ELC and the catalytic domain of S1 and/or the link between the ELC and RLC domains were flexible, we would expect a smaller stiffness and thus a smaller force. Thus, the properties of the light chains may affect the flexural rigidity of the lever arm, thereby regulating the force produced by a particular myosin isoform.

The establishment of laser trap technologies to measure directly the force and work produced by a single myosin molecule (6, 50) and systems that allow genetic engineering of the molecular motor myosin to produce myosins with different lever arm lengths (this paper) should allow critical testing of whether force production is inversely proportional to the lever arm length squared, as predicted by the elastic lever arm model.

The same approaches should allow testing of the concept that the nature of the light chains modulates the spring constant of the elastic lever arm and therefore the amount of force that can be produced by different isoforms of myosin,

which have different light chains. Indeed, even skeletal myosin binds two alternate forms of RLC, for reasons that have been unclear. Moreover, myosin light chains are altered by post-translational modifications, such as phosphorylation in the case of smooth muscle myosin and *Dictyostelium* myosin (for a review, see ref. 51) and binding of Ca^{2+} in the case of scallop myosin (52). One goal then is to use molecular genetics and laser trap technology to gain detailed molecular information about the physiological relevance of altered myosin types.

We thank members of the Spudich laboratory for stimulating discussions and advice, and K. Zaita for technical assistance. This work is supported by a Human Frontier Science Program short-term fellowship to T.Q.P.U. and National Institutes of Health Grant GM33289 to J.A.S.

1. Itakura, S., Yamakawa, H., Toyoshima, Y. Y., Ishijima, A., Kojima, T., Harada, Y., Yanagida, T., Wakabayashi, T. & Sutoh, K. (1993) *Biochem. Biophys. Res. Commun.* **196,** 1504–1510.
2. Rayment, I., Rypniewski, W., Schmidt-Base, K., Smith, R., Tomchick, D., Benning, M., Winkelmann, D., Wesenberg, G. & Holden, H. (1993) *Science* **261,** 50–58.
3. Xie, X., Harrison, D. H., Schlichting, I., Sweet, R. M., Kalabokis, V. N., Szent-Gyorgyi, A. G. & Cohen, C. (1994) *Nature (London)* **368,** 306–312.
4. Cooke, R., Crowder, M. S., Wendt, C. H., Bamett, V. A. & Thomas, D. D. (1984) *Adv. Exp. Med. Biol.* **170,** 413–427.
5. Vibert, P. & Cohen, C. (1988) *J. Muscle Res. Cell Motil.* **9,** 296–305.
6. Finer, J. T., Simmons, R. M. & Spudich, J. A. (1994) *Nature (London)* **368,** 113–119.
7. Ishijima, A., Harada, Y., Kojima, H., Funatsu, T., Higuchi, H. & Yanagida, T. (1994) *Biochem. Biophys. Res. Commun.* **199,** 1057–1063.
8. Miyata, H., Hakozaki, H., Yoshikawa, H., Suzuki, N., Kinoshita, K., Jr., Nishizaka, T. & Ishiwata, S. (1994) *J. Biochem. (Tokyo)* **115,** 644–647.
9. Molloy, J. E., Burns, J. E., Kendrick-Jones, J., Tregear, R. T. & White, D. C. S. (1995) *Nature (London)* **378,** 209–212.
10. Tokunaga, M., Sutoh, K. & Wakabayashi, T. (1991) *Adv. Biophys.* **27,** 157–167.
11. Wakabayashi, K., Tokunaga, M., Kohno, I., Sugimoto, Y., Hamanaka, T., Takezawa, Y., Wakabayashi, T. & Amemiya, Y. (1992) *Science* **258,** 443–447.
12. Highsmith, S. & Eden, D. (1993) *Biochemistry* **32,** 2455–2458.
13. Whittaker, M., Kubalek, E. M. W., Smith, J. E., Faust, L., Milligan, R. A. & Sweeney, H. L. (1995) *Nature (London)* **378,** 748–751.
14. Jontes, J. D., Kubalek, E. M. W. & Milligan, R. A. (1995) *Nature (London)* **378,** 751–753.
15. Irving, M., St Claire Allen, T., Sabido-David, C., Craik, J. S., Brandmeier, B., Kendrick-Jones, J., Corrie, J. E. T., Trentham, D. R. & Goldman, Y. E. (1995) *Nature (London)* **375,** 688–691.
16. Uyeda, T. Q. P., Kron, S. J. & Spudich, J. A. (1990) *J. Mol. Biol.* **214,** 699–710.
17. Harada, Y., Sakurada, K., Aoki, T., Thomas, D. D. & Yanagida, T. (1990) *J. Mol. Biol.* **216,** 49–68.
18. Spudich, J. A. (1994) *Nature (London)* **372,** 515–518.
19. Lowey, S., Waller, G. S. & Trybus, K. M. (1993) *Nature (London)* **365,** 454–456.
20. Uyeda, T. Q. P. & Spudich, J. A. (1993) *Science* **262,** 1867–1870.
21. Waller, G. S., Ouyang, G., Swafford, J., Vibert, P. & Lowey, S. (1995) *J. Biol. Chem.* **270,** 15348–15352.
22. Ausubel, F., Brent, R., Kingston, R. E., Moore, D. D., Seidman, J. G., Smith, J. A. & Struhl, K., eds. (1994) *Current Protocols in Molecular Biology* (Current Protocols, New York).
23. Egelhoff, T. T., Manstein, D. J. & Spudich, J. A. (1990) *Dev. Biol.* **137,** 359–367.
24. Ruppel, K. M., Uyeda, T. Q. P. & Spudich, J. A. (1994) *J. Biol. Chem.* **269,** 18773–18780.
25. Sussman, M. (1987) *Methods Cell Biol.* **28,** 9–29.
26. Egelhoff, T. T., Titus, M. A., Manstein, D. J., Ruppel, K. M. & Spudich, J. A. (1991) *Methods Enzymol.* **196,** 319–334.
27. Spudich, J. A. & Watt, S. (1971) *J. Biol. Chem.* **246,** 4866–4871.
28. Margossian, S. S. & Lowey, S. (1982) *Methods Enzymol.* **85,** 55–71.
29. Gordon, D. J., Yang, Y. Z. & Korn, E. D. (1976) *J. Biol. Chem.* **251,** 7474–7479.
30. Bradford, M. M. (1976) *Anal. Biochem.* **72,** 248–254.
31. Perrie, W. T. & Perry, S. V. (1970) *Biochem. J.* **119,** 31–38.
32. Kron, S. J. & Spudich, J. A. (1986) *Proc. Natl. Acad. Sci. USA* **83,** 6272–6276.
33. Toyoshima, Y. Y., Kron, S. J., McNally, E. M., Niebling, K. R., Toyoshima, C. & Spudich, J. A. (1987) *Nature (London)* **328,** 536–539.
34. Maita, T., Yajima, E., Nagata, S., Miyanishi, T., Nakayama, S. & Matsuda, G. (1991) *J. Biochem. (Tokyo)* **110,** 75–87.
35. Warrick, H. M., DeLozanne, A., Leinwand, L. A. & Spudich, J. A. (1986) *Proc. Natl. Acad. Sci. USA* **83,** 9433–9437.
36. Stein, L. A., Schwarz, Jr., R. P., Chock, P. B. & Eisenberg, E. (1979) *Biochemistry* **18,** 3895–3909.
37. Rosenfeld, S. S. & Taylor, E. W. (1984) *J. Biol. Chem.* **259,** 11920–11929.
38. Burke, M. & Reisler, E. (1977) *Biochemistry* **16,** 5559–5563.
39. Wells, J. A. & Yount, R. G. (1979) *Proc. Natl. Acad. Sci. USA* **76,** 4966–4970.
40. Huxley, A. F. & Simmons, R. M. (1971) *Nature (London)* **233,** 533–538.
41. Kron, S. J., Toyoshima, Y. Y., Uyeda, T. Q. P. & Spudich, J. A. (1991) *Methods Enzymol.* **196,** 399–416.
42. Kishino, A. & Yanagida, T. (1988) *Nature (London)* **334,** 74–76.
43. Rayment, I., Holden, H. M., Whittaker, M., Yohn, C. B., Lorenz, M., Holmes, K. C. & Milligan, R. A. (1993) *Science* **261,** 58–65.
44. Feynman, R. P., Leighton, R. B. & Sands, M. (1964) *The Feynman Lectures on Physics* (Addison-Wesley, Reading, MA), Vol. 2.
45. Gittes, F., Mickey, B., Nettleton, J. & Howard, J. (1993) *J. Cell Biol.* **120,** 923–934.
46. Hagerman, P. J. (1988) *Annu. Rev. Biophys. Biophys. Chem.* **17,** 265–286.
47. Bagshaw, C. R. (1993) *Muscle Contraction* (Chapman & Hall, London), 2nd Ed.
48. Higuchi, H., Yanagida, T. & Goldman, Y. E. (1995) *Biophys. J.* **69,** 1000–1010.
49. Howard, J. & Ashmore, J. F. (1987) *Hearing Res.* **23,** 93–104.
50. Finer, J., Mehta, A. & Spudich, J. A. (1995) *Biophys. J.* **68,** 291s–297s.
51. Tan, J. L., Ravid, S. & Spudich, J. A. (1992) *Annu. Rev. Biochem.* **61,** 721–759.
52. Houdusse, A. & Cohen, C. (1996) *Structure* **4,** 21–32.